A THREE-DIMENSIONAL FRICTIONAL STRESS ANALYSIS OF DOUBLE-SHEAR BOLTED WOOD JOINTS

Shen-Haw Ju

Professor
Department of Civil Engineering
National Cheng-Kung University
Tainan, Taiwan, Republic of China 70101

and

Robert E. Rowlands

Professor
Department of Mechanical Engineering
University of Wisconsin
Madison, WI 53706

ABSTRACT

The three-dimensional stresses in bolted wood connections are evaluated and the results compared with those from two-dimensional analyses. Elastic bolts, bolt/hole clearance, and geometric variations are accounted for, as are the effects of side members. While the two- and three-dimensional results agree reasonably well with each other for relatively short bolts (thin members), contact stresses become extremely large and highly three-dimensional for proportionally longer bolts (thick members) and/or with decreased friction. Under such conditions, plane-stress assumptions are inadequate. Ability to include friction is facilitated by using special contact elements that have a symmetrical stiffness matrix.

Keywords: Finite elements, three dimensional, contact stresses, bolted joints, fasteners, connectors, wood.

INTRODUCTION

Connections are often the "Achilles heel" of a wood structure. Fastener failure can present serious economic and human consequences, but inadequate stress information has hampered development of better design methodologies. Experimental, numerical, and analytical difficulties have limited most bolted-joint studies to plane stress and rigid bolts. However, many joints have significant three-dimensional (3-D) effects (Serabian 1991; Rothert et al. 1992; Sundarraj et al. 1995; Williams 1995; Hart-Smith 1995; Cheng and Lee 1995; Chen et al. 1995; Barbero et al. 1995; Fung and Smart 1994, 1997; Soltis and Wilkinson 1987; Patton-Mallory 1996; Bauman 1998). While Wilkinson and Rowlands (1981), Hyer et al. (1987), Rodd (1988), Kim et al. (1998), and Zang et al. (2000) have noted the desire to include bolt friction, this is the first 3-D numerical stress analysis of bolted wood connections that accounts for both friction and side members. Comparing two-dimensional (2-D) with 3-D results demonstrates here that to ignore 3-D effects can overpredict performance of bolted wood joints.

This paper provides a three-dimensional finite element analysis (FEA) of the stresses in three-member, single-bolted wood connectors and compares them with those based on plane stress. Friction between the deformable steel bolt and connected wood members is incorporated. The materials are assumed to behave linear-elastically. Variations in bolt clearance and relative geometry are accounted for, whereas effects of wood crushing, wood clamping, bolt heads, nuts, or washers (Iarve and Witney 1999) are not included. Frictional

bolt/wood contact is handled numerically with special contact elements (Ju and Rowlands 1999; Ju et al. 1995). The three-dimensional effects become extremely significant as the bolt's aspect ratio exceeds about four. Interestingly, the European Yield Model predicts, and it has been observed experimentally, that the normalized bearing strength of wood connectors decreases for bolt aspect ratios greater than about four (Soltis and Wilkinson 1987; Wood Handbook 1999).

Present attention focuses on the bolt/wood contact stresses. The analyses rely heavily on efficient two- and three-dimensional frictional contact elements. Only the most pertinent finite element model (FEM) aspects are included here and the reader is directed to the References (Ju and Rowlands 1999; Ju et al. 1995) for details. Results demonstrate the importance of accounting for friction, bolt clearance, and relative bolt length.

The only published three-dimensional FEM stress analyses of bolted wood fasteners known to the authors are those by Patton-Mallory 1996 and Bauman 1998. Patton-Mallory studied frictionless pin-loaded wood plates, including nonlinear constitutive behavior. Her FEM model does not include side members. Bauman analyzed up to four co-linear bolt-loaded holes, but virtually all of his results are for zero friction.

FINITE ELEMENT ANALYSIS

This analysis uses a recently developed 3-D frictional contact element (Ju and Rowlands 1999). This element contains one contact node and four target nodes. Moreover, it can be implemented into an existing FEM program without having to modify the main program or solution method.

The governing matrix equation of the penalty method at a certain iteration is (Ju et al. 1995; Ju and Rowlands 1999).

$$(K + K_s)dx = F_{ext} - F_{int} - Fs_{int}, \quad (1)$$

where dx = incremental displacement vector between two successive iterations, K = total tangent stiffness matrix of the bodies (i.e.,

contactor and target), K_S = total stiffness matrix of all contact elements, F_{ext} = external force vector, F_{int} = internal force vector of contactor and target bodies, and Fs_{int} = internal normal and frictional force vector of the contact elements. Quantities K and F_{int} of Eq. (1) are assembled using typical elements.

This study assumes Coulomb friction at the contacting curved surface between the bolt and wood,

$$F = f_s - \mu f_n \quad (2)$$

where f_n and f_s are the magnitudes of normal and frictional forces (both positive) and μ is the frictional coefficient. If $F = 0$, the element slides. If $F < 0$, the element sticks. For node-to-node contact and providing three degrees of freedom in the local directions, the element stiffness matrix at a point can be formulated as

$$\begin{Bmatrix} df_s \\ df_{sl} \\ df_n \end{Bmatrix} = [K_{local}] \begin{Bmatrix} dU \\ dV \\ dW \end{Bmatrix} \quad (3)$$

where

$$[K_{local}] = [K_{stick}] = \begin{bmatrix} k & 0 & 0 \\ 0 & k & 0 \\ 0 & 0 & k \end{bmatrix} \quad \text{for sticking.} \quad (4)$$

Although $[K_{local}]$ is unsymmetrical when sliding occurs, this unsymmetrical matrix can be replaced by the following symmetric matrix:

$$[K_{local}] = [K_{slide}]$$

$$= \begin{bmatrix} \mu^2 k & 0 & \mu k \\ 0 & k_v & 0 \\ \mu k & 0 & k \end{bmatrix} \quad \text{for sliding.} \quad (5)$$

Quantity f_{sl} is the internal friction force, dU is the relative displacements between two successive iterations in the last tangential direction (direction of the frictional stress at the end of last iteration), dV is the relative displacement due to the change of the tangential direction between the present and last iterations (dU is perpendicular to direction dV), dW is the relative displacement in the normal direc-

Point P_1 = Contact node at last iteration;
Point P_2 = Contact node at current iteration;
Point C_1 = Contact position at last iteration
Point C_2 = Contact position at current iteration
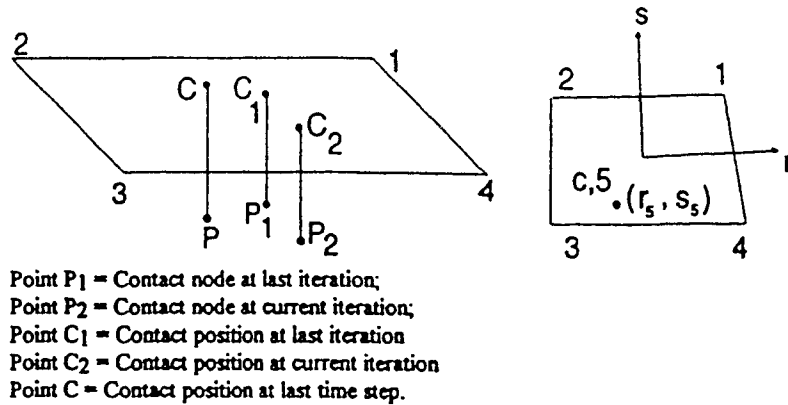Point C = Contact position at last time step.

FIG. 1.   Five-node contact element and natural coordinates (r-s).

tion between two successive iterations, k is a large input penalty constant, and k_v is the penalty constant for dV. One can approximate k_v by the average value of df_s/dU of all the iterations during this force step.

This symmetric solution scheme is efficient for contact problems having both sticking and sliding modes since it is twice as fast as the unsymmetrical solution scheme, and the amount of computer memory needed is typically reduced significantly. The above stiffness matrices can be transformed into global coordinates. In order to solve node-to-surface contact problems, a linear transformation matrix is used to transform the node-to-node stiffness matrix to the five-node (node-to-surface) stiffness matrix (Fig. 1) in Eq. (6):

$$\mathbf{K}_5 = \mathbf{K} \begin{bmatrix} N_1N_1 & N_1N_2 & N_1N_3 & N_1N_4 & -N_1 \\ N_2N_1 & N_2N_2 & N_2N_3 & N_2N_4 & -N_2 \\ N_3N_1 & N_3N_2 & N_3N_3 & N_3N_4 & -N_3 \\ N_4N_1 & N_4N_2 & N_4N_3 & N_4N_4 & -N_4 \\ -N_1 & -N_2 & -N_3 & -N_4 & 1 \end{bmatrix}$$

(6)

where $N_1 = (1 + r_5)(1 + s_5)$, $N_2 = (1 - r_5)(1 + s_5)$, $N_3 = (1 - r_5)(1 - s_5)$, $N_4 = (1 + r_5)(1 - s_5)$, and r_5 and s_5 are the natural coordinates of node 5. K is the global stiffness matrix for sticking, separating, or sliding modes, respectively, and is evaluated from Eqs. (4) or (5).

If the current coordinates of points 1

through 5 of the target surface and the contact modes (sticking, sliding, or separating) are known, Eq. (6) can be used to provide the tangent stiffness matrix of the node-to-surface contact element.

Knowing the displacements, one can evaluate the local internal forces, F_n and F_s at node 5 of the contact element. The normal force is

$$F_n = kW,$$

(7)

where W is the normal displacement. The friction force is

$$F_s = kU + (\mathbf{u}_1 \cdot \mathbf{u})F_{s1} \quad \text{for sticking,}$$

(8)

and

$$F_s = \mu F_n \qquad\qquad \text{for sliding,}$$

(9)

where $\mathbf{u}$ and $\mathbf{u}_1$ are the unit direction vectors parallel to the displacement U of this iteration and the last iteration, respectively, and F_{s1} is the internal frictional force at the end of the previous increment.

Local internal forces, F_n and F_s, at node 5 can be found from the above equations. Global internal forces at nodes 1 to 5 of the target element can be calculated using Eqs. (10) and (11). Adding the element internal forces to the global force vector enables one to obtain FSint in Eq. (1), i.e.,

$$\begin{Bmatrix} F_{x5} \\ F_{y5} \\ F_{z5} \end{Bmatrix} = [\mathbf{u}^T - \mathbf{v}^T] \begin{Bmatrix} F_s \\ F_n \end{Bmatrix} \qquad (10)$$

$$\begin{Bmatrix} F_{x1} \\ F_{x2} \\ F_{x3} \\ F_{x4} \end{Bmatrix} = -F_{x5} \begin{bmatrix} N_1 \\ N_2 \\ N_3 \\ N_4 \end{bmatrix}, \quad \begin{Bmatrix} F_{y1} \\ F_{y2} \\ F_{y3} \\ F_{y4} \end{Bmatrix} = -F_{y5} \begin{bmatrix} N_1 \\ N_2 \\ N_3 \\ N_4 \end{bmatrix},$$

and

$$\begin{Bmatrix} F_{z1} \\ F_{z2} \\ F_{z3} \\ F_{z4} \end{Bmatrix} = -F_{z5} \begin{bmatrix} N_1 \\ N_2 \\ N_3 \\ N_4 \end{bmatrix}, \qquad (11)$$

where $\mathbf{v}$ is a unit vector parallel to V.

If W is negative, then node 5 has separated from the 4-node target surface. Under such condition, the penalty constant and internal forces of the contact element are both set to zero. If $W \geq 0$, one then checks to see whether sliding or sticking occurs. Sticking is first assumed. Thus, if $F_s < \mu F_n$, sticking occurs; if $F_s \geq \mu F_n$, one has sliding. Equations (6) through (11) provide the current tangent stiffness matrix and contact current forces of a node-to-plane contact element at each iteration once the coordinates are updated to their current values.

FASTENER MODELING

Figure 2 is a schematic of a single-bolted, three-member fastener. Each side member of the joint has a thickness equal to half that of the middle member. Both middle and side wood members are subjected to uniform applied tension, S, far from the bolt. Analyses account for bolt clearance and bolt/member friction ($\mu = 0.7$). Typically with wood fasteners, bolt tension and friction between the middle- and side members are ignored. Effects due to bolt heads, nuts, and washers are omitted, which enables bolts to be analyzed as elastic pins. Dimensions of Fig. 2, including the diametral bolt clearance of 1.59 mm (1/16

in.), are representative of the wood industry (Wood Handbook 1999; Wilkinson 1986).

Figure 3a shows a 3-D discretization of bolted connector of Fig. 2. Half-, rather than quarter-, FEM models were prepared to provide for subsequent computational flexibilities (top half of the middle member, one side member and half of the elastic pin). There are 32 brick elements along the half circle on the contact side of the hole in addition to the 3-D five-node contact elements between the pin and plate. A side member and the middle half-member both have six elements in their thickness direction.

It is informative to compare two- and three-dimensional results and see under what conditions plane-stress ceases to be realistic. The 2-D model of Fig. 2b, which is identical to that of the in-plane surface of the 3-D mesh, uses a rigid pin, four-node quadrilateral isoparametric elements and 2-D three-node contact elements between the bolt and a wood member.

The FEA models were loaded incrementally using a total of four load steps. From three to 15 iterations were used per load increment; the number of iterations needed per increment increases with increasing member thickness. Bolts are elastic in the 3-D analyses and rigid in the 2-D models. Both the 2-D and 3-D FEA models include the incompatible modes (Wilson et al. 1973) to overcome the inaccuracy of the bending effect due to the linear isoparametric formulation.

FASTENER GEOMETRY AND MATERIAL

The three-member wood joint of Fig. 2 was analyzed over the relative thickness range (bolt aspect ratio) $1 \leq L/d \leq 8$, based on a bolt/pin diameter of $d = 1.91$ cm (0.75 in.). This L/d range is typical of that used in timber design (Soltis and Wilkinson 1987; National Design Specification for Wood Construction 1997; Wood Handbook 1999). For example, bolting three 2-by-6s together with 1.9-cm (¾ in.) diameter bolts results in a L/d of six. Unless stated otherwise, Sitka spruce wood prop-
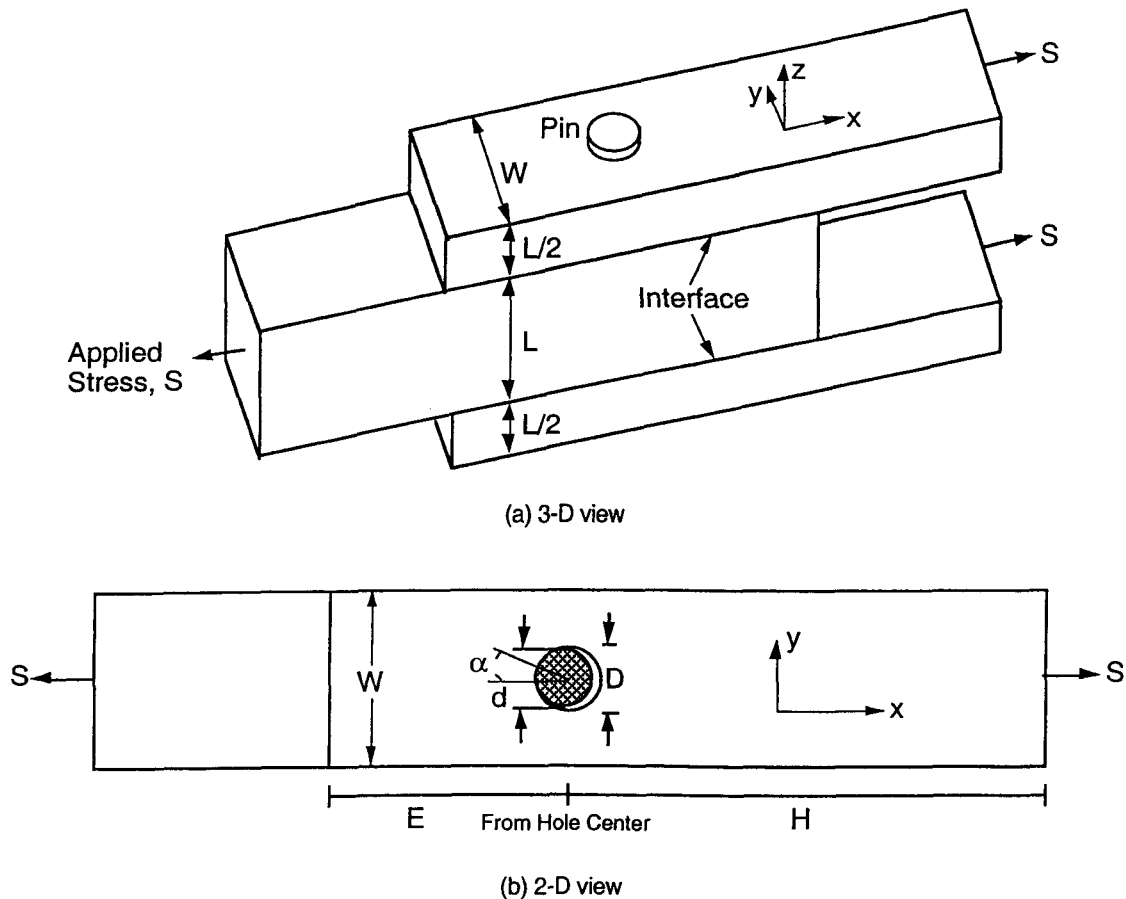
Fig. 2. Three-member bolted wood joint [d = 1.905 cm (0.75 in.) and 2.032 cm (0.8 in.), D = 2.063 cm (13/16 in.), d/D = 0.92 and 0.99, W/d = 3 and 6, E/d = 4 and 7, H/d = 8, and L = 1.91 cm, 3.81 cm, 7.62 cm, and 15.24 cm, respectively].

erties are used, with the grain in the loading direction and the radial wood direction parallel to the axis of the hole/bolt, Table 1 (Rahman et al. 1991; Wood Handbook 1999; Wilkinson and Rowlands 1981). All analyses are for a hole diameter of D = 2.06 cm (13/16 in. = 0.813 in.) and most are for d = 1.91 cm, i.e., d/D = 0.92. Timber structures typically employ a diametral bolt clearance of between 0.8 mm (1/32 in.) to 1.59 mm (1/16 in.) (Wood Handbook 1999; Wilkinson 1986).

RESULTS

Stresses

Figure 4 shows the computed contact (normal, radial) stress distributions along the length of the bolt hole in the top (outside) member of Fig. 2 caused by the bolt bearing against the spruce and for various values of L/d. With reference to Figs. 2 and 3, the vertical centerline of these images of Fig. 4 coincides with the axis of the hole, and the bottom edge of the images is the interface between the top (side) and middle members of the joint. The width of the images corresponds to the hole diameter, D, and the horizontal lines are element interfaces. The stress contours of Fig. 4 are based on a far-field stress of S = 1.38 MPa (200 psi) applied to each of the middle- and side members of Fig. 2.

Variations in the normal contact stress along the length of the bolt (i.e., through the wood
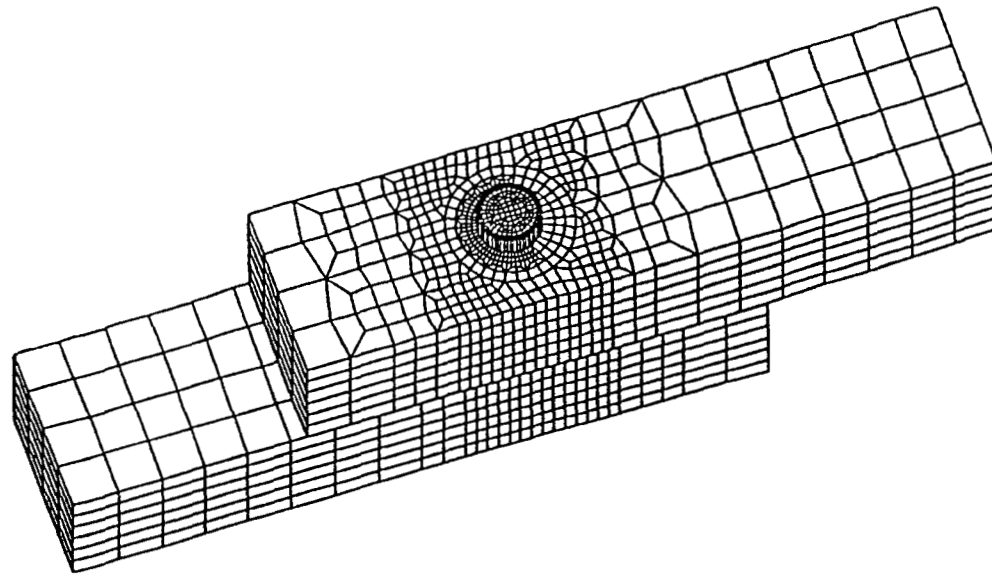
(a) 3-D view of the finite element mesh
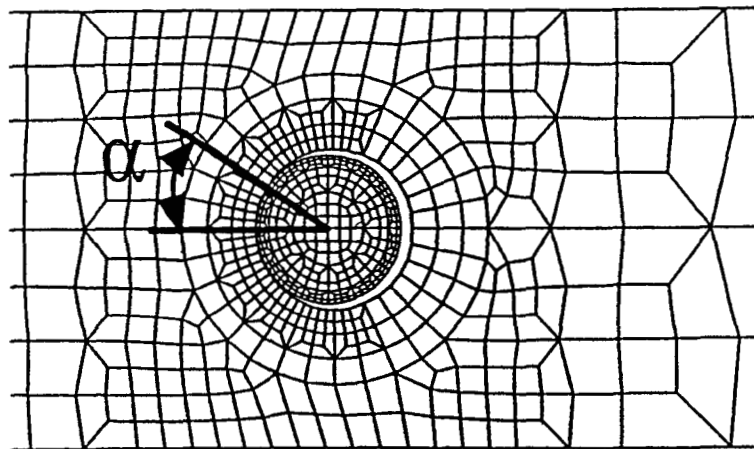
(b) 2-D view of the mesh near the pin-joint region

FIG. 3.   Finite element models of bolted joint of Fig. 2.   (3-D model: 8936 eight-node isoparametric brick elements having 11,382 nodes, plus 3248 five-node contact elements; 2-D model: rigid pin, 450 four-node quadrilateral isoparametric elements having 539 nodes, plus 108 three-node contact elements).

thickness) with L/d are evident in Fig. 4, particularly for L/d > 2. For increased L/d, the bolt deflects sufficiently that it bears heavily against the wood of the side member which abuts the middle member but loses contact with the hole surface toward the top of the outer member. As L/d increases, the contact stress in the top (outside) member concentrates near its bottom interface with the middle member. It is consequently unnecessary to show the unloaded upper portion of the top, outside member for L/d = 8 in Fig. 4d. The

TABLE 1. *Elastic properties.*

Sitka spruce

E_{xx} = 13.8 GPa (2e^6 psi)

E_{yy} = 0.55 GPa (0.08e^6 psi)

E_{zz} = 1.1 GPa (0.16e^6 psi) ν_{xy} = 0.48

                                            ν_{yz} = 0.24

G_{xy} = 0.83 GPa (0.12e^6 psi) ν_{zx} = 0.04

G_{yz} = 0.04 GPa (0.006e^6 psi)

G_{zx} = 0.88 GPa (0.13e^6 psi)

Steel

     E = 207 GPA (30e^6 psi) ν = 0.25

35.6 MPa compressive stress level of Fig. 4c approaches a strength parallel to the grain of 38 MPa for Sitka spruce (Wood Handbook 1999).[1]

Bolt deflection has implications beyond rendering the stresses three-dimensional. Hart-Smith (1995) discusses reduced fastener strength caused by bolt bending, including loss of contact over part of the outer members (as occurs in Fig. 4). Washers, heads, or nuts of bent bolts can (if present) also dig into the outer joint members, causing damage. Williams (1995) reports nuts actually being sheared from bolts that were bent during fastener loading.

Based on member width W = 5.7 cm (W/d = 3) and the stress of 1.38 MPa (200 psi) applied to each of the middle and side members of Fig. 2, Table 2 shows the actual load applied to the spruce joint for each of the values of L/d of Fig. 4. Table 2 also predicts fastener capacity according to the European Yield Model (Soltis and Wilkinson 1987), the proportional limit bolt load and the design load recommended by the National Design Specification (NDS) (1997). The values of Table 2 based on the European Yield Model are the lesser of the mode I (spruce bearing failure),

---

[1] Douglas-fir has a corresponding compressive strength of 50 MPa, while that of Kaneelhart can approach 120 MPa. Compressive proportional limits are in the range of 30–35 MPa, 40–45 MPa, and 80–110 MPa for Sitka spruce, Douglas fir and Kaneelhart, respectively (Wood Handbook 1999; Rahman et al. 1991; Patton-Mallory 1996).
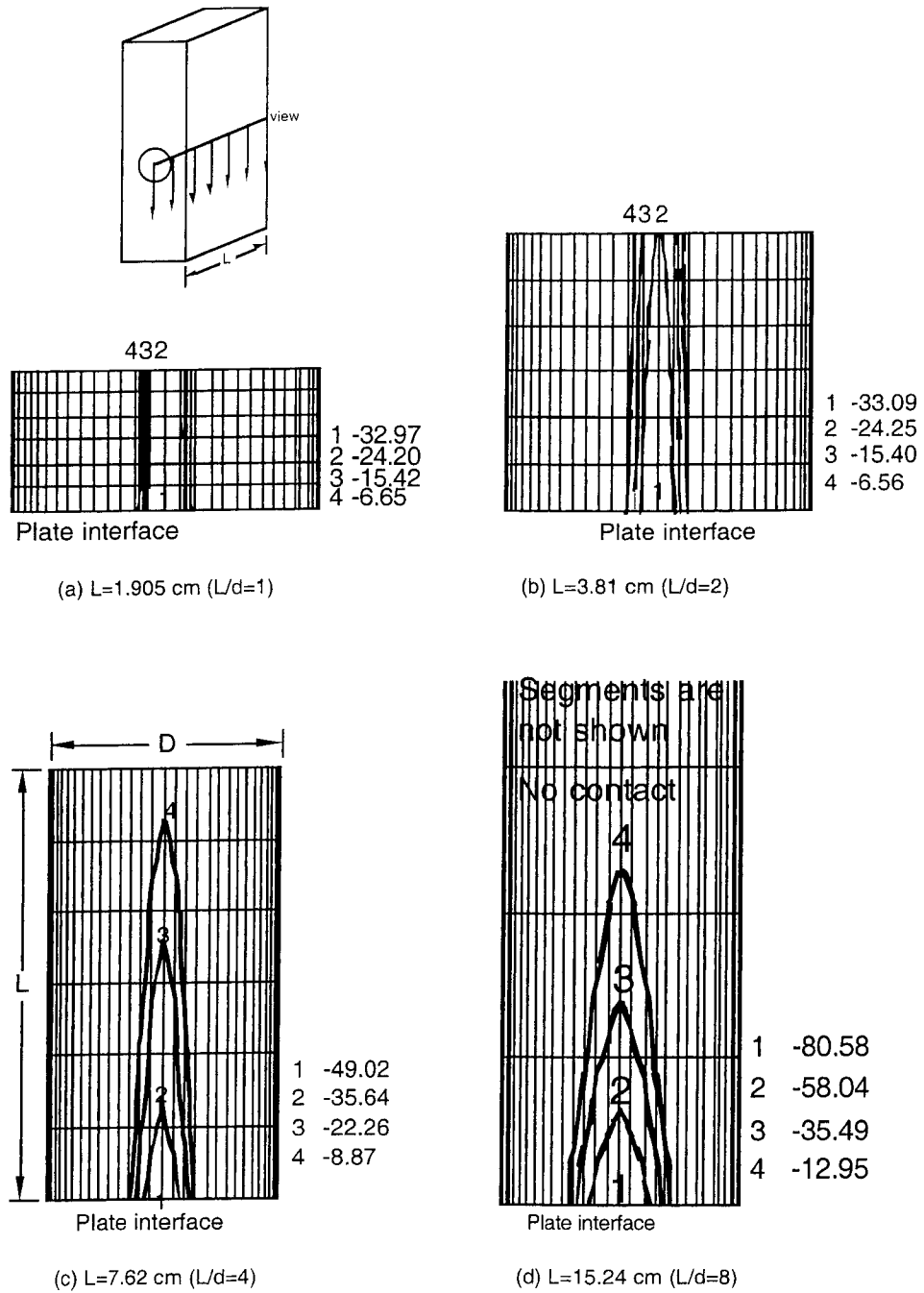
III$_s$ (bolt develops plastic hinge in the middle member only), or IV (bolt develops plastic hinges in the middle and side members) from Table 3. The NDS-predicted design strengths of Table 2 are similarly the minimum respective values from Table 4.

Data of Table 2 indicate that the joints of Fig. 4 are loaded well below strengths predicted by the European Yield Model, as well as below the proportional limit bolt loads and below their NDS design values. Notwithstanding this, and while the maximum stresses of Fig. 4 are concentrated toward the middle member, a portion of the hole surface of Fig. 4d is predicted to be stressed significantly beyond the compressive proportional limit for Sitka spruce. Figure 4a shows uniform bearing loading against the wood (would probably lead ultimately to mode I failure), whereas Fig. 4d suggests that, for L/d = 8, ultimate failure might involve bolt yielding (modes III$_s$ or IV). However, the relatively low bolt stresses (to be noted subsequently) here would favor any current structural degradation of an actual spruce connector (of this geometry loaded to 12 kN) involving at least some wood damage. In this particular case, the elastically-predicted stresses of Figs. 4 and 5 exceed the proportional limit of the spruce when L/4 ≥ 4, which corresponds to when predicted connector failure would shift from mode I to yielding of a 310 MPa yield-strength bolt, Tables 3 and 4. Replacing the present bolt, whose assumed yield strength is 310 MPa (45 ksi), with one having a yield strength of 965 MPa (140 ksi; NDS 1997) would increase the European Yield Model mode IIIs predictions of Table 3 to 53–57 kN (for all L/d considered here) and the mode IV prediction from 42 kN to 75 kN. Similarly, using a 965 MPa (140 ksi) yield-strength bolt would increase the predicted mode IIIs and mode IV design values of Table 4 to at least 16.6 kN and 23.4 kN, respectively.

The stresses of Fig. 5 are for the same case (L/d = 8) as that of Fig. 4d but for an applied far-field fastener stress of S = 0.69 MPa (100 psi). The contact stress in Fig. 5 continues to be highly three-dimensional. The connector of

FIG. 4.   Normal contact stress contours (MPa) between steel bolt and side member of double-shear spruce joint (d = 1.91 cm, d/D = 0.92, W/d = 3, E/d = 4, μ = 0.7, and S = 1.38 MPa).

TABLE 2. *Loading and predicted strength of three-member bolted spruce joints* ($W = 5.7$ cm, $d = 1.905$ cm).

L/d	Applied load (kN) ($S = 1.379$ MPa)	Predicted strength (kN)		
		European yield model, F_y**	Prop. limit bolt load*	NDS design value, Z**
1	1.5	12	6.9	3
2	3	24	13.7	6
4	6	31	21	9.7
8	12	41	22	12.8

* Based on Sitka spruce compressive strength parallel to the grain of 37.8 MPa (5480 psi) (Wood Handbook 1999).

** Based on Sitka spruce bearing strength parallel to the grain of 33 MPa (4800 psi) (National Design Specifications for Wood Construction 1997).

Fig. 4d is twice as highly loaded as is that of Fig. 5 ($P = 12$ kN vs. 6 kN), although the radial stress at the interface between the side (top) and the middle plate of Fig. 4d is only 1.6 times that of Fig. 5. This is indicative of stress nonlinearities in such contant problems.[2]

Figure 6 compares the normal contact stress distributions on the curved surface of the bolt hole (3-D FEA) at the interface between the top (outside) and middle members (Figs. 2–4) with that from the 2-D FEA. While the 2-D analysis is reasonable for relatively small L/d, it is inadequate for L/d $\geq$ 4. Computed stresses of individual cases associated with Fig. 6 have been normalized by the far-field applied fastener stress of $S = 1.38$ MPa (200 psi). Appropriate stress summation for the 2-D anal-

[2] A joint identical to that of Fig. 5 (L/d = 8, S = 0.69 MPa) was also analyzed for Kaneelhart middle and side members. Moduli used for the Kaneelhart are twice those of Table 1, whereas the Poisson's Ratios of Table 1 were again utilized (Wood Handbook 1999). The predicted maximum normal contact stress in a Kaneelhart side member (at its interface with middle member) is 70 MPa. This compares with a proportional limit in the grain direction for this species of 80–110 MPa.

TABLE 3. *Strength (kN), F_y, of three-member bolted spruce joints as predicted by the European Yield Model**

Mode	L/d			
	1	2	4	8
$I_m = I_s$	12	24	48	96
III_s	32	30	31	41
IV	←————— 42* —————→			

* Based on a bending yield stress for the bolt of 310 MPa (45 ksi) (Soltis and Wiklinson 1987).

TABLE 4. *Design values (kN) Z of three-member bolted spruce joints as predicted by the National Design Specification (NDS) for Wood Construction**

Mode	L/d			
	1	2	4	8
$I_m = I_s$	3	6	12	24
III_s	9.9	9.4	9.7	12.8
IV	←————— 13.3* —————→			

* Based on a bending yield stress for the bolt of 310 MPa (45 ksi).

ysis of Fig. 6 agrees with the magnitude of the applied load within 2.4%.[3]

The stresses of Fig. 4 compare with a nominal bearing stress (total applied load across projected bolt area) of 4.1 MPa (600 psi). Clearance causes the bolt to contact only a relatively small arc portion of the hole surface,

[3] An application of this FEM scheme to double-shear bolted steel joints shows an agreement of 1%.

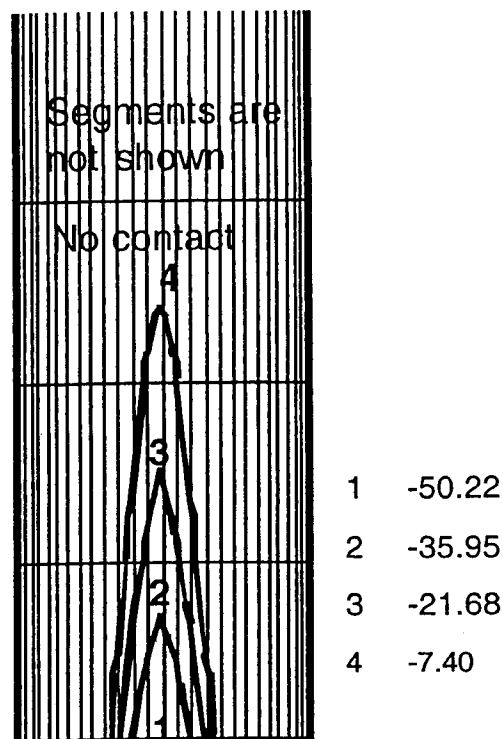| 1	-50.22
2	-35.95
3	-21.68
4	-7.40

FIG. 5. Normal contact stress contours (MPa) between steel bolt and side member of double-shear spruce joint for L/d = 8 and S = 0.69 MPa (d = 1.91 cm, d/D = 0.92, W/d = 3, E/d = 4, and $\mu = 0.7$).
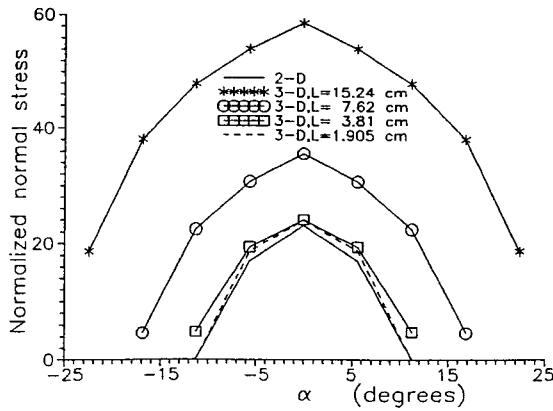
FIG. 6. Normalized normal bolt/spruce contact stresses at interface between side and middle members by each of two- and three-dimensional FEA [d = 1.91 cm, d/D = 0.92, W/d = 3, E/d = 4, μ = 0.7, and S = 1.38 MPa (200 psi); 2-D analyses use rigid bolt while 3-D analyses use steel bolt; normalized normal stress = normal contact stress/S].
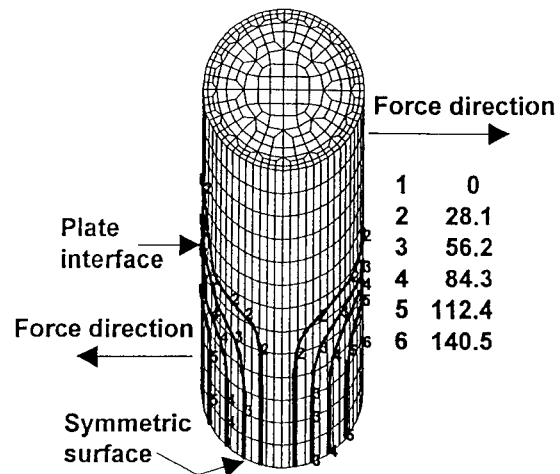

FIG. 7. Von Mises stress contours (MPa) of steel bolt of the bolted spruce connection of Fig. 4d (L = 15.24 cm, L/d = 8, d = 1.91 cm, d/D = 0.92, W/d = 3, E/d = 4, μ = 0.7, and S = 1.38 MPa).

although the maximum arc length of surface contact increases with increased L/d, Figs. 4 and 6. The small contact area (d/D = 0.92) contributes to stress concentrations as high as 23 for the 2-D analysis of Fig. 6.

The maximum contact stress of 31.5 MPa by the 2-D plane stress analysis of Fig. 6 approximates the measured compressive proportional limit for Sitka spruce of 30 MPa (Rahman et al. 1991). However, and notwithstanding that the joint is loaded below the predicted yield strengths of Table 2, the 3-D elastic FEA would predict localized contact stresses as high as 80 MPa (Figs. 4d and 6).

Figure 7 shows the calculated von Mises (effective) stress contours in the top-half of the steel bolt for connector and loading of Fig. 4d, i.e., L/d = 8, the most severe case considered. The normal contact stresses of Fig. 4d bear against the upper left-hand side of the bolt of Fig. 7, whereas the stress contours on the lower right-hand side of the bolt are due to the compressive loading of the top-half of the middle wood member of Figs. 2 and 3. The stresses in the lower left-hand portion of this top-half of the bolts are a manifestation of the bolt bending along its longitudinal (vertical) axis. The maximum value of the von Mises

stress of 140.5 MPa (20 ksi) in the bolt is only 45% of the steel's yield stress of 310 MPa (45 ksi). This collaborates data of Table 2 that the bolt response is elastic.

Effects of variations in friction and geometry

Results of Figs. 4 through 7 are for μ = 0.7, hole diameter D = 2.06 cm, bolt diameter d = 1.91 cm (d/D = 0.92), width W = 5.7 cm (W/d = 3), end distance E = 7.6 cm (E/d = 4), bolt aspect ratio 1 ≤ L/d ≤ 8, and diametral bolt clearance of 1.6 mm (1/16 in.). The consequences of changes in friction, relative geometry, and bolt/hole clearance for spruce fasteners are demonstrated in Fig. 8. The variation ratio of Fig. 8 is the value of the maximum normal contact stress on the hole boundary of the top (side) member computed by the 3-D FEA divided by the corresponding maximum contact stress evaluated by the 2-D FEA. Increasing values of the variation ratio are therefore a measure of increasing 3-D effects. The clearance coefficient, C, of Fig. 8 is calculated from the expression C = (D − d)/d. Clearance, C, is consequently 1/12 for d = 1.91 cm (0.75 in.) and D = 2.06 cm (13/16 in.), and C = 1/64 by making d = 2.03 cm (0.80 in.), giving d/D = 0.98, i.e., a decrease
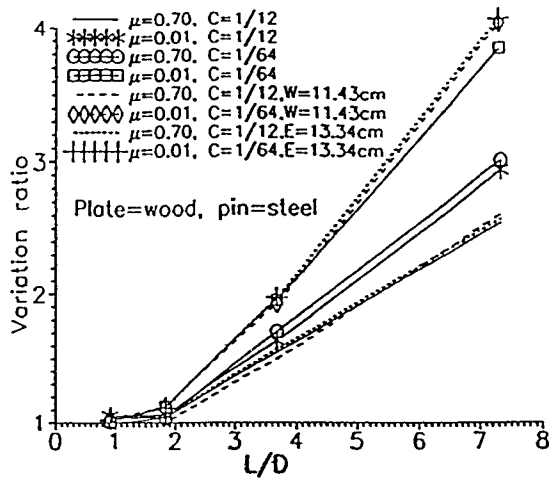
Fig. 8. Effects of changes in friction, width, end distance, and bolt clearance on the extent of three-dimensionality of the contact stress between steel bolt and side spruce member [D = 2.06 cm (13/16 in.) and S = 1.38 MPa (200 psi)]. If W or E is not shown in legend, the default values (W= 5.72 cm and E = 7.62 cm) are used. (Variation ratio is the value of the maximum normal contact stress on the hole boundary of the top (side) member as computed by 3-D FEA divided by the maximum contact stress evaluated by 2-D FEA; C = (D-d)/d).

in diametral clearance from 1.6 mm (1/16 in.) to 0.8 mm (~1/32 in.).

These changes in variation ratio with L/D of Fig. 8 further demonstrate the three-dimensional significance of the contact stresses along the thickness direction (z-direction). Increases in the variation ratio imply an increasingly nonuniform stress distribution through the thickness. While increasing either member width (from W = 5.72 cm to W = 11.43 cm; W/D = 2.8 to 5.5) or end distance (from E = 7.62 to E = 13.34 cm; E/D = 3.7 to 6.5) has little impact on the stresses, decreased friction (from μ = 0.7 to μ = 0.1) or decreased clearance (from C = 1/12 to 1/64) increases the stress triaxiality.[4] Moreover, stresses become

[4] Values of E/d ≥ 7 are recommended for parallel-to-grain tensile loading of softwoods and E/d ≥ 4 for hardwoods (Wood Handbook 1999). Patton-Mallory (1996) measured an 8–10% reduction in the maximum load of tensile bolt-loaded single plates (W/d = 3) of Douglas fir having 2 ≤ L/d ≤ 5 and E/d = 4 compared with those having E/d = 7, but no such load degradation occurred with L/d ≥ 7.

more three-dimensional as L/D increases, the effects being almost linear with L/D for L/D > 2. The observed increase in stress triaxiality with decreased bolt clearance might be partly associated with related changes in bolt end-restraint provided by the side plates. Using μ = 0.7 is typical of the wood industry.

The present study concentrates on the stresses in outside members of double-shear bolted wood connections in which all three members have identical orthotropic properties and whose side plates are each half as thick as the middle plate. Elastically predicted highest stresses in the middle plate are comparable in magnitude to those in the side plates.

All stress profiles reported in this paper are from actual nodal information. No smoothing procedure was used.

DISCUSSION

Three-dimensional bolt/hole contact stresses in three-member, bolted wood connections are determined and results compared with those for plane stress. The model accounts for friction, bolt elasticity, bolt/hole clearance, and geometric variations. Effects of bolt heads, nuts, or washers are not included. Linear elasticity is assumed. Except when joint members are relatively thin (i.e., small bolt aspect ratio, L/d), the contact stress tends to be highly three-dimensional.

At least for 1 ≤ L/d ≤ 8, increasing either fastener width beyond W/d = 3 or end distance beyond E/d = 4 has little influence on the extent of contact stress triaxiality of wood connections. However, changes in friction, L/d, or bolt clearance can be significant. Decreasing friction or bolt clearance, or increasing L/d, can render the stresses so three-dimensional that plane-stress analyses are inadequate. Maximum contact stresses from 3-D FEA can be twice as large as those based on plane stress.

The present information regarding W/d and E/d agrees with other results for wood joints loaded parallel to the grain. Wilkinson and Rowlands (1981), Hirai and Swada (1982), Soltis and Wilkinson (1987), and Chiang and

Rowlands (1991) demonstrated that most relevant stresses and connector strength are independent of W/d for W/d > 3.

Bolted wood fasteners of typical L/d, and loaded below design values, can exhibit appreciable nonuniform bolt/hole contact stress in the thickness direction. Local stresses can readily become nonlinear/inelastic, something a 2-D analysis might not predict. Although it is reasonable to assume plane stress and rigid bolts in wood fasteners having L/d $\leq$ 2, the contact stress becomes appreciably three-dimensional for L/d $\geq$ 4. Monitoring the shape of the bolt during connector loading verifies it deforms, but the bolts remain comparatively stiff for relatively thin members (L/d < 2). Under such conditions, the bolt's circular cross-section changes, but little bolt bending occurs.

Present findings are compatible with those by Patton-Mallory (1996), Bauman (1998), and Fung and Smart (1997). The latter reports increased local stresses in riveted joints due to increased member thickness or decreased friction. That some stresses sometimes increase with decreased friction might suggest (and acknowledging the added numerical complexity of accounting for friction) ignoring friction will automatically predict a worst situation and therefore provide a conservative design. As discussed below, the authors caution against jumping to such a conclusion, but rather encourage seeking a better understanding of the role friction plays. The need to fully understand the three-dimensional nature of the stresses in bolted joints extends beyond wood connections. Hart-Smith (1995), while recognizing the desire to restrict bearing stresses, discusses expanded use of mechanical fasteners in thick aerospace composite structures.

The effects of friction between bolts/pins and the connected material on stress and strength are not totally established (Patton-Mallory et al. 1997; Wilkinson and Rowlands 1981; Chiang and Rowlands 1991; Eriksson 1986). A 2-D FEA of bolted composites by Kim et al. (1998) shows better agreement between predicted and measured strength when

friction is accounted for numerically, and Pierron et al. (2000) report predicted strains in pin-jointed woven composites agree with measured values provided friction is included numerically. Test data by Rodd (1988) show that friction at the bolt/wood interface increases connector strength, and Hyer et al. (1987) and Zang et al. (2000) mention the importance of including frictional effects when analyzing bolted joints.

Since bolted (or nailed) joints virtually always involve side members, it is important to fully model their participation in the stress analysis. Among other considerations, side members influence bolt bending and consequently the stresses in the wood.

Present results imply that at least local compressive wood damage (yielding, failure, nonlinear/inelastic behavior) can occur at connector loads below the NDS design loads and well below load levels predicted to initiate yielding of the bolt. Linear elasticity is assumed here, but the computed compressive stresses sometimes exceed the proportional compressive strength of spruce. While wood responds reasonably linear-elastically in tension parallel and transverse to the grain, and in shear parallel to the grain, it is nonlinear in compression parallel to the grain. FEA and measured moiré data illustrate that accounting for nonlinear compressive constitutive response parallel to the grain can reduce the computed normal stress in the wood immediately beneath the pin by 40% compared with that based on linear elasticity (Rahman et al. 1991). Particularly for the higher values of L/d, some local wood damage (crushing) can be expected to occur. This would cause the actual angle of bolt/wood contact to be greater than predicted elastically.

Relatively few 3-D analyses of bolted joints in orthotropic materials involve bolt clearance and bolt/hole friction. To do so using traditional FEM models/codes can pose numerical difficulties. The authors are unaware of any previously published 3-D FEM stress analyses of bolted wood connections that combine the effects of side members, bolt clearance, and

bolt/hole friction. Ability to conduct such studies is facilitated here by using special frictional contact elements. The present analysis involves a statically-loaded wood joint whose materials are assumed to behave linear-elastically. The reliability of the frictional contact element employed has been demonstrated for several static and dynamic problems involving extensive amounts of sliding and for a variety of constitutive behaviors (Ju and Rowlands 1999). The general numerical approach is therefore applicable to wood connections involving more complicated loading, geometry or material behavior.

Numerical models of wood connectors are extremely useful and their comprehensiveness is being improved. This paper emphasizes the bolt/wood contact stresses. However, one should not ignore potential effects of variations in L/d and side members on the perpendicular-to-grain tensile stresses along the end region of a connector or the consequences of multiple bolts. At higher loads, particularly if intended to predict connector strength, effects of material nonlinearity and damage should be included. The influences of bolt clearance and friction on stress triaxiality warrant further study.

CONCLUSIONS

This is the first 3-D FEM stress analysis of bolted wood joints known to the authors that models both friction and side members. At least for $1 \leq L/d \leq 8$, increasing either fastener width beyond $W/d = 3$ or end distance beyond $E/d = 4$ appears to have little influence on the extent of bolt/wood contact stress triaxiality of three-member bolted wood joints. While two- and three-dimensional stress analyses of such connectors agree with each other for relatively short bolts (thin members), the contact stresses can become extremely large and highly three-dimensional for proportionally longer bolts (thick members). Decreasing friction or bolt clearance, or increasing L/d, may render the stresses so three-dimensional that plane-stress results are totally inadequate.

Results indicate that local stresses can become nonlinear (inelastic) at loads below design values, and well below predictions by the European Yield Model—something a two-dimensional analysis might well not predict. Models that ignore 3-D effects may significantly overpredict the performance of bolted wood connectors.

REFERENCES

BAUMAN, B. J. 1998. A numerical and experimental investigation of mechanical connections. Ph.D. thesis, University of Wisconsin, Madison, WI.

BARBERO, F. J., R. LUCIANO, AND E. SACCO. 1995. Three-dimensional plate and contact/friction elements for laminated composite joints. Computers and Structures 54(4):689–703.

CHEN, W. H., S. S. LEE, AND J. T. YEH. 1995. Three-dimensional contact stress analysis of a composite laminate with bolted joint. Composite Structures 30:287–297.

CHENG, W. H., AND S. S. LEE. 1995. Numerical and experimental failure analysis of composite laminates with bolted joints under bending. Composite Mater. 29(1): 15–36.

CHIANG, Y. J., AND R. E. ROWLANDS. 1991. Finite element analysis of mixed-mode fracture of bolted joints in composites. J. Composite Tech. Res. 13(4):227–235.

ERIKSSON, L. J. 1986. Contact stresses in bolted joints of composite laminates. Composite Structures 6:57–75.

FUNG, C. P., AND J. SMART. 1994. An experimental and numerical analysis of rivetted single lap joints. J. Aerospace Eng., I Mech E, 208:79–90.

———, AND ———. 1997. Riveted single lap joints. Part I: A numerical parametric study. J. Aerospace Eng., I Mech E, 221(G):13–27.

HART-SMITH, L. J. 1995. An engineer's viewpoint on design and analysis of aircraft structural joints. J. Aerospace Eng., I Mech E, 209(G2):105–129.

HIRAI, T., AND M. SWADA. 1982. The effect of margins on

the lateral resistance of bolted joints loaded parallel to the grain. J. Japan Wood Res. Soc. 28(3):137–142.

HYER, M. W., E. C. KLANG, AND D. E. COOPER. 1987. The effects of pin elasticity, clearance and friction on the stresses in a pin-loaded orthotropic plate. J. Composite Mat. 21:190–206.

IARVE, E. V., AND T. J. WHITNEY. 1999. Three-dimensional stress analysis in composite laminates with elastic fastener and washer clamp-up. American Soc. Composites Mtg., Sept. 27–29.

JU, S. H., AND R. E. ROWLANDS. 1999. A three-dimensional frictional contact element whose stiffness matrix is symmetric. ASME J. Appl. Mech. 66:460–468.

———, J. J. STONE, AND R. E. ROWLANDS. 1995. A new symmetric contact element stiffness matrix for frictional contact problems. Computers and Structures 54(2):289–301.

KIM, S. J., J. S. HWANG, AND J. H. KIM. 1998. Progressive failure analysis of pin-loaded laminated composites using penalty finite-element method. AIAA J. 36(1):75–80.

NATIONAL DESIGN SPECIFICATION FOR WOOD CONSTRUCTION. 1997. American Forest and Paper Association, Washington, DC.

PATTON-MALLORY, M. 1996. The three-dimensional mechanics and failure of single bolt wood connections. Ph.D. thesis, Colorado State University, Fort Collins, CO.

———, P. J. PELLICANE, AND F. W. SMITH. 1997. Modeling bolted connections in wood. Review. ASCE J. Structural Eng. 123(8):1054–1062.

PIERRON, F., F. CERISIER, AND M. GREDIAC. 2000. A numerical and experimental study of woven-composite pin-joints. J. Comp. Mater. 34(12):1028–1054.

RAHMAN, M. U., Y. J. CHIANG, AND R. E. ROWLANDS. 1991. Stress and failure analysis of double-bolted joints in Douglas fir and Sitka spruce. Wood Fiber Sci. 23(4): 567–589.

RODD, P. D. 1988. Timber joints made with improved circular dowel fasteners. Pages 26–37 *in* Vol. 1 Proc. Int'l Conference on Timber Engr., Seattle. Forest Products Research Society, Madison, WI.

ROTHERT, H., N. GEBBEKEN, AND B. BINDER. 1992. Nonlinear three-dimensional finite element contact analysis of bolted connections in steel frames. Intl. J. Numerical Methods in Eng. 34:303–318.

SERABIAN, S. M. 1991. The effects of nonlinear interlaminar shear behavior on the modeling accuracy of [(0/ 90)₃,0]ₛ and [(+45/−45)]₂₅ pin-loaded laminates. J. Composites Technol. Res., JCTRER. 13(4):236–248.

SOLTIS, L. A., AND T. L. WILKINSON. 1987. Bolted-connection design, Tech. Rep. No. FPL-GTR-54, Forest Products Laboratory, Madison, WI.

SUNDARRAJ, N., B. DATTAGURU, AND R. RAMAMURTHY. 1995. Analysis of a double shear lap joint with interference fit pin. Computers and Structures 55(2):357–363.

WILKINSON, T. L. 1986. Load distribution among bolts parallel to load. ASCE J. Structural Eng. 112(4):835–852.

———, AND R. E. ROWLANDS. 1981. Analysis of mechanical joints in wood. Exp. Mech., November. 21(4):408–414.

WILLIAMS, G. D. 1995. Personal communication.

WILSON, E. L., R. L. TAYLOR, W. P. DOHERTY, AND J. GHABOUSSI. 1973. Incompatible displacement models. Pages 43–57 *in* S. J. Fenves, N. Perrone, A. R. Robinson, and W. C. Schnobrich, eds. Numerical and computer method in structural mechanics. Academic Press, New York, NY.

WOOD HANDBOOK. 1999. USDA Forest Products Laboratory, Madison, WI.

ZANG, C., R. GANESAN, AND S. V. HOA. 2000. Effects of friction on three-dimensional contact stresses in pin-loaded laminated composites. J. Composite Mater. 34(16):1382–1415.